Quaternary Research 78 (2012) 130–138

Contents lists available at SciVerse ScienceDirect

Quaternary Research

journal homepage: www.elsevier.com/locate/yqres

Aerobic degradation of organic carbon inferred from dinoflagellate cyst decomposition in Southern Ocean sediments

Monika Kupinska [a,*], Oliver Sachs [c], Eberhard J. Sauter [b], Karin A.F. Zonneveld [a]

[a] Fachbereich 5-Geowissenschaften, Postfach 330440, 28334 Bremen, Germany
[b] Alfred Wegener Institute for Polar and Marine Research, Am Handelshafen 12, 27570 Bremerhaven, Germany
[c] Eberhard & Partner AG, General Guisan-Strasse 2, 5000 Aarau, Switzerland

ARTICLE INFO

Article history:
Received 22 October 2010
Available online 30 May 2012

Keywords:
Organic-walled dinoflagellate cysts
Oxygen
Organic carbon
Degradation

ABSTRACT

Organic carbon (OC) burial is an important process influencing atmospheric CO_2 concentration and global climate change; therefore it is essential to obtain information on the factors determining its preservation. The Southern Ocean (SO) is believed to play an important role in sequestering CO_2 from the atmosphere via burial of OC. Here we investigate the degradation of organic-walled dinoflagellate cysts (dinocysts) in two short cores from the SO to obtain information on the factors influencing OC preservation. On the basis of the calculated degradation index *kt*, we conclude that both cores are affected by species-selective aerobic degradation of dinocysts. Further, we calculate a degradation constant *k* using oxygen exposure time derived from the ages of our cores. The constant *k* displays a strong relationship with pore-water O_2, suggesting that decomposition of OC is dependent on both the bottom- and pore-water O_2 concentrations.

Introduction

The Southern Ocean (SO) is believed to play an important role in modulating atmospheric CO_2 levels and hence to influence global climate changes. Different reconstructions show that atmospheric CO_2 during the last glacial period was reduced by ~80 ppm in comparison to pre-industrial modern times (e.g. Siegenthaler and Wenk, 1984; Moore et al., 2000). However, the mechanism responsible for lowering CO_2 level is not yet well understood. For example, one hypothesis assumes that sea-ice expansion caused permanent surface water stratification south of the Antarctic Polar Front (PF) which resulted in reduced vertical mixing, thus preventing the ventilation of CO_2-rich deep water and CO_2 release to the atmosphere (e.g. François et al., 1997; Sigman and Boyle, 2000). Another hypothesis links lower CO_2 levels with carbon sequestration in marine sediments as a result of higher primary productivity caused by enhanced dust delivery to the SO during the last glacial stage (e.g. Martin et al., 1990). However, high primary productivity alone does not influence carbon sequestration. It is the export production and more importantly the organic carbon (OC) burial in marine sediments that can remove carbon from the global carbon cycle on a longer time scale. It is assumed that only 0.1% of the OC produced is ultimately preserved within ocean sediments, whereas the major part is oxidised to CO_2, H_2O and nutrients, thereby introducing carbon back to the sea-water and the atmosphere (Hedges et al., 1997). Therefore it is important to estimate the degradation rates of OC as accurately as possible.

A factor that strongly affects OC preservation is O_2 availability which determines the respiratory types of benthic organisms, with anaerobic micro-organisms being slightly less efficient than aerobic micro-organisms and micro- and macro-fauna. Redox oscillations may enhance degradation by promoting symbiosis of aerobes and anaerobes (e.g. Aller, 2001; Aller and Blair, 2006). For an adequate estimation of OC degradation it is therefore important to have detailed information about the redox conditions at the ocean floor in the geological past.

Recently, a method to estimate past bottom-water O_2 concentrations has been suggested (Zonneveld et al., 2007). This method is based on the observation that species-selective degradation of organic-walled dinoflagellate cysts (dinocysts) under oxic conditions is strongly related to the bottom-water O_2 concentration (Zonneveld et al., 2001; 2007). The production of one dinocyst taxon in the upper waters is assumed to be strongly related to the production of other dinocysts, but species-selective degradation of this specific dinocyst taxon is however independent from degradation/preservation of other taxa. This information can be used to decouple preservation from productivity and to estimate past bottom-water O_2 (Versteegh and Zonneveld, 2002).

As with other marine OC, dinocysts reaching the sea floor can vary from extremely labile to highly refractory, and their degradation is based on the same premises as the decay of the entire OC pool (e.g. Zonneveld et al., 2008). The degradation of individual OC components is considered to be a first-order process depending on the degradation constant *k* and the oxygen exposure time *t* (Middelburg, 1989;

* Corresponding author at: Geosciences Faculty, University of Szczecin, Mickiewicza 18, 70-383 Szczecin, Poland.
E-mail address: monika.kodrans-nsiah@univ.szczecin.pl (M. Kupinska).

0033-5894/$ – see front matter © 2012 University of Washington. Published by Elsevier Inc. All rights reserved.
doi:10.1016/j.yqres.2012.04.001

Hedges and Prahl, 1993; Canfield, 1994; Hartnett et al., 1998; Sun et al., 2002; Keil et al., 2004). However, the degradation of the OC pool as a whole is much more complex, with the proportion of refractory OC increasing over time as result of, for example (a) biodegradation rates decreasing with decreasing OC quality, (b) oxidative polymerisation, and in the anoxic zone of the sediments also sulphurisation transferring labile OC towards the refractory pool and (c) no degradation of archaeal and bacterial OC.

For individual OC components, O_2 is often considered to influence degradation as a function of t (Rabouille and Gaillard, 1991; Arthur et al., 1998). If this were the case, a linear relation between the degradation constant k and O_2 could be found. Recent studies suggest that for dinocysts a more complex relation exists between O_2 and degradation rates, suggesting that the complex biomolecules forming the dinocysts might not degrade according to a first-order process (Zonneveld et al., 2007). In an attempt to obtain further insight into the relationship between dinocyst degradation and O_2, we compared the degradation rates of dinocysts with in-situ measurements of pore-water O_2 in two well-dated short cores from the Atlantic sector of the SO. Here we discuss the effects of both upper ocean environmental conditions as well as pore water O_2 on the preservation of the dinocysts. Furthermore, we discuss how far the taphonomy of dinocysts might form a model for OC degradation and preservation.

Materials and methods

The cores PS65/705 and PS65/703 (Table 1) were taken during *R/V Polarstern* expedition ANT XXI/4 in 2004 in the high-productivity belt along the PF and in a region of relatively lower surface productivity south of the PF respectively (Fig. 1).

For sediment sampling a multiple corer with a core diameter of 10 cm was deployed (Barnett et al., 1984). Apparently undisturbed sediment cores were obtained.

The deposits of core 705 can be divided into three parts. The upper part (0–13 cm) consisted of inhomogeneous, brown, extremely soft, diatomaceous sediment; the middle part (13–21 cm) contained inhomogeneous brown diatomaceous mud, the lower part (21–28 cm) was composed of homogeneous grey to white mud. The sediment of core 703 consisted of homogeneous light brown diatomaceous mud throughout (0–20 cm).

For dinocyst analysis, the upper 25 and 10 cm of sediment cores 705 and 703 were sampled at 0.5 and 2.5 cm resolution, respectively. The material was dried overnight at 60°C. Samples were then treated with cold 10% HCl and cold 40% HF in order to remove carbonates and silicates, respectively. After each acid treatment, samples were carefully neutralised with KOH. The digested samples were sieved through a 20 μm precision sieve (Stork Veco, mesh 508), treated with ultrasonic vibration and sieved again. The sample residues were centrifuged (8 min, 3500 rpm) and concentrated to 1.0 or 1.5 ml. Part of each residue was mixed in glycerine jelly and insulated from the air on a glass microscope slide with paraffin wax. For each sample at least 100 (100–229) dinocysts were counted. An exception was sample 5.0–7.5 cm of the 703 core for which, after counting of all available material, only 83 dinocysts were found. The counts were subsequently used to calculate dinocyst concentrations by dividing the number of cysts counted by the sample dry weight analysed. Dinocyst fluxes were derived from dinocyst concentrations and sedimentation rates. The reliability of counting results and percentage

Table 1
Station list (site labels are abbreviated in the text: 703 for PS65/703 and 705 for PS65/705).

Site label	Date	Latitude (S)	Longitude (E)	Depth (m)
PS65/703	29.04.2004	52°35.12′	09°00.19′	3330
PS65/705	30.04.2004	49°00.06′	12°15.32′	4293

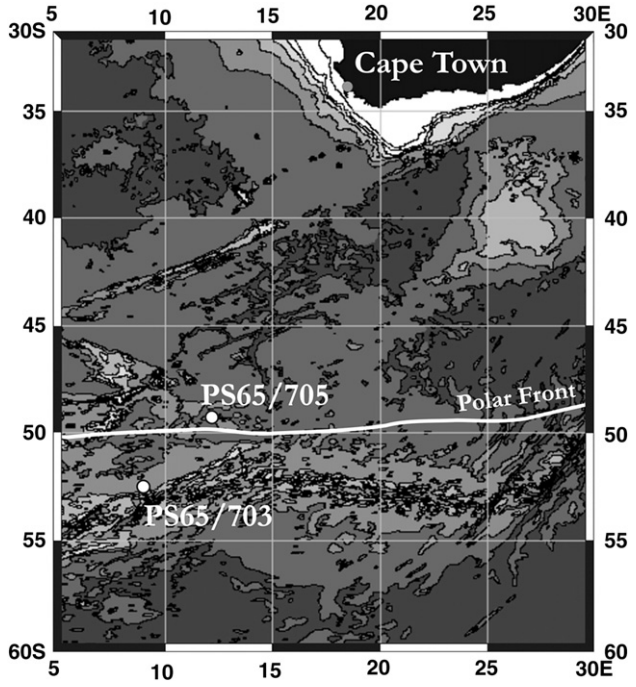

Figure 1. Core sites and PF locations in the Atlantic sector of the Southern Ocean.

estimation errors (Tables 2 and 3) were calculated using half-width of two-sided 95 percent confidence bounds (van der Plas and Tobi, 1965; Howarth, 1998). Errors for the percentages<1 were not computed.

In order to obtain information on the dinocyst preservation the *kt* index was calculated for each sample according to the equation given in Versteegh and Zonneveld (2002):

$$kt = \ln\left(X_i/X_f\right) \tag{1}$$

where k is the degradation constant for sensitive (labile) dinocysts (S-cysts), t is the oxygen exposure time, X_f is the observed dinocyst flux (cyst/cm^2/yr) and X_i is the initial dinocyst flux calculated from the fixed relationship between fluxes of S-cysts and resistant (refractory) dinocysts (or R-cysts; Table 4; Zonneveld et al., 2007):

$$Flux_{S-cysts} = 68 * Flux_{R-cysts} \tag{2}$$

Lower index values mean better preservation and higher values mean greater degradation of the dinocysts.

The degradation constant k was calculated using Eq. (1) assuming that in the oxygenated samples t is equal to the age of the samples. For the anoxic samples of the 705 core t was calculated dividing O_2 penetration depth by sedimentation rate. The O_2 penetration depth of 10 cm was inferred from the measured O_2 profile under assumption that it is roughly stable through time. Oxygen exposure time of the anoxic sediments could be prolonged by the deposit's re-exposure to O_2 via such mechanisms as bioturbation (Hulthe et al., 1998). Traces of bioturbation in our cores were virtually absent; therefore we expect only a minor effect of re-exposure on estimated t.

Sample age and sedimentation rates were calculated from ^{210}Pb data using the Constant Flux Model of Robbins (1978). According to this model, the age of a given sediment layer can be derived from the equation:

$$T = 1/\lambda * \ln(\Gamma_z/\Gamma_0) \tag{3}$$

where T is the age of the bottom of a given sediment layer z in years, Γ_z is the inventory of $^{210}Pb_{excess}$ below depth z, Γ_0 is the total

https://doi.org/10.1016/j.yqres.2012.04.001 Published online by Cambridge University Press

Table 2
Number of dinocysts counts, relative abundances and half-width of two-sided 95 percent confidence bound on observed dinocysts percentages in the 705 core. A — *Brigantedinium* spp., B — *S. antarctica*, C — *N. labyrinthus*, D — *I. aculeatum*, E — *I. sphaericum*, F — *D. chathamensis*.

Sample depth (cm)	Dinocysts counts							Relative abundances (%)						Half-width of two-sided 95% confidence bound on observed %					
	Total	A	B	C	D	E	F	A	B	C	D	E	F	A	B	C	D	E	F
0.0–0.5	117.0	64.0	25.0	6.0	1.0	14.5	2.0	54.7	21.4	5.1	0.9	12.4	1.7	9.0	7.0	3.5	–	5.5	1.5
0.5–1.0	172.5	82.5	34.5	15.0	4.0	29.5	2.0	47.8	20.0	8.7	2.3	17.1	1.2	7.5	6.0	4.0	1.8	5.5	0.9
1.0–2.0	108.0	55.0	28.5	5.0	1.0	16.5	0.0	50.9	26.4	4.6	0.9	15.3	0.0	9.0	8.0	3.5	–	6.5	–
2.0–3.0	121.5	61.0	26.0	7.0	3.0	16.0	1.0	50.2	21.4	5.8	2.5	13.2	0.8	9.0	7.0	4.0	2.0	6.0	–
3.0–4.0	100.5	64.0	21.5	5.0	1.0	8.0	0.0	63.7	21.4	5.0	1.0	8.0	0.0	10.0	8.0	3.5	1.0	5.5	–
4.0–5.0	126.0	69.0	27.5	8.0	4.0	12.5	3.0	54.8	21.8	6.3	3.2	9.9	2.4	9.0	7.0	4.0	2.0	5.0	1.8
5.0–6.0	109.0	33.5	41.0	6.0	2.0	19.5	1.0	30.7	37.6	5.5	1.8	17.9	0.9	8.5	9.0	4.0	1.5	7.5	–
6.0–7.0	114.5	5.01	22.0	15.0	2.0	20.5	1.0	44.5	19.2	13.1	1.7	17.9	0.9	9.0	7.5	6.0	1.5	7.0	–
7.0–8.0	135.0	57.0	28.0	16.0	3.0	25.0	1.0	42.2	20.7	11.9	2.2	18.5	0.7	8.5	7.0	5.0	1.7	6.5	–
8.0–9.0	144.5	68.5	30.0	8.0	6.0	23.0	3.0	47.4	20.8	5.5	4.2	15.9	2.1	8.5	6.5	3.5	3.0	6.0	1.5
9.0–10.0	186.0	115.5	22.0	14.0	6.0	18.0	4.5	62.1	11.8	7.5	3.2	9.7	2.4	7.0	4.5	3.0	2.0	4.0	1.7
10.0–11.0	154.5	60.5	18.0	19.0	1.5	37.0	6.5	39.2	11.7	12.3	1.0	23.9	4.2	8.0	5.0	5.0	0.9	6.5	3.0
11.0–12.0	105.0	50.5	13.5	14.5	7.0	15.5	0.0	48.1	12.9	13.8	6.7	14.8	0.0	10.0	6.0	6.0	5.0	7.0	–
12.0–13.0	134.0	32.0	24.0	20.0	7.0	36.0	6.5	23.9	17.9	14.9	5.2	26.9	4.9	7.0	6.5	6.0	3.1	7.5	3.1
13.0–14.0	206.5	88.0	46.5	22.0	3.0	28.5	5.0	42.6	22.5	10.7	1.5	13.8	2.4	7.0	5.5	4.0	1.0	5.0	1.7
14.0–15.0	139.0	62.5	34.5	5.0	5.0	27.5	1.0	45.0	24.8	3.6	3.6	19.8	0.7	8.0	7.0	2.0	2.0	7.0	–
15.0–16.0	215.5	147.5	50.5	5.0	0.0	9.0	2.0	68.4	23.4	2.3	0.0	4.2	0.9	6.5	6.0	1.6	–	2.5	–
16.0–17.0	116.0	65.0	36.0	4.0	0.0	10.0	0.0	56.0	31.0	3.4	0.0	8.6	0.0	9.0	8.0	2.4	–	5.0	–
17.0–18.0	128.5	67.0	37.5	3.0	2.0	14.0	1.0	52.1	29.2	2.3	1.6	10.9	0.8	8.5	7.5	1.7	1.2	5.0	–
18.0–19.0	118.0	68.5	36.5	2.0	0.0	7.0	1.0	58.1	30.9	1.7	0.0	5.9	0.8	8.5	8.0	1.2	–	3.5	–
19.0–20.0	121.0	61.0	30.0	5.0	0.0	19.0	1.0	50.4	24.8	4.1	0.0	15.7	0.8	9.0	7.5	3.0	–	6.0	–
20.0–21.0	110.5	59.0	25.0	5.0	3.0	12.5	0.0	53.4	22.6	4.5	2.7	11.3	0.0	9.0	7.5	3.5	2.0	5.5	–
21.0–22.0	117.5	65.0	22.5	4.0	2.0	21.0	3.0	55.3	19.1	3.4	1.7	17.9	2.6	9.0	7.5	2.5	1.5	6.5	2.0
22.0–23.0	116.5	58.5	25.5	2.0	2.0	21.0	2.0	50.2	21.9	1.7	1.7	18.0	1.7	9.5	7.5	1.5	1.5	6.5	1.5
23.0–24.0	113.5	27.5	19.0	5.0	5.0	39.0	7.0	24.2	16.7	4.4	4.4	34.4	6.2	8.0	6.5	3.0	3.0	8.5	4.0
24.0–25.0	124.0	88.0	25.0	2.0	1.0	6.0	0.0	71.0	20.2	1.6	0.8	4.8	0.0	8.0	7.5	1.2	–	3.5	–

inventory of $^{210}Pb_{excess}$ in sediment and λ is the decay rate constant for ^{210}Pb equal to 0.0311 a^{-1} (Ferdelman et al., 2006). Gamma analysis for the determination of ^{210}Pb (47 keV), ^{40}K (1460 keV) and the ^{226}Ra daughter products ^{214}Pb (295 and 352 keV) and ^{214}Bi (609 keV), were performed on dried and powdered samples that were sealed at least 21 days prior to measurements to ensure secular equilibrium between ^{226}Ra and daughter products ^{214}Pb, ^{214}Bi.

Total organic carbon (TOC) content was determined by pyrolysis and oxidation at 2000°C in an induction furnace within an oxygen stream, followed by infrared carbon dioxide detection (Leco Carbon Determinator CS-125). Prior to analysis the material was treated with HCl in order to remove carbonates. TOC content was calculated as weight percentage of dry sediment.

Benthic O_2 microprofiles were measured in situ by means of an autonomous deep-sea microprofiler (Unisense A/S, Denmark) deployed in combination with a free-fall lander system. The profiler was equipped with five oxygen sensors and a formation factor probe (resistivity sensor). Clark-type oxygen sensors (Unisense A/S) with tip diameters of ~25 μm and a stirring sensitivity<2%, pre-calibrated according to Sauter et al. (2001), were lowered through the sediment water interface into the sediment with a vertical resolution of 0.5 mm during 5–6 h at the sea floor.

Results

Sample ages and sedimentation rates

The results of ^{210}Pb analysis show that the 25 cm long core 705 spans an interval of 170 yr and the 10 cm of the 703 core corresponds to a period of 142 yr. The cores were taken in 2004, and therefore the tops of both cores are assumed to be deposited in that year. This allows us to allocate the ages (in yr AD) to each sample (Fig. 2).

The sedimentation rates inferred from estimated ages of the samples range generally between 0.03 and 1.56 cm/yr, which is much higher than average sedimentation rates for the open ocean. Such high sedimentation rates could be related to the cores' location in the PF zone which is known to be an area with extraordinarily high primary production and rapid export of particles to the sea floor.

Table 3
Number of dinocysts counts, relative abundances and half-width of two-sided 95 percent confidence bound on observed dinocysts percentages in the 703 core. A — *Brigantedinium* spp., B — *S. antarctica*, C — *N. labyrinthus*, D — *I. aculeatum*, E — *I. sphaericum*.

Sample depth (cm)	Dinocyst counts						Relative abundances (%)					Half-width of two-sided 95% confidence bound on observed %				
	Total	A	B	C	D	E	A	B	C	D	E	A	B	C	D	E
0.0–0.5	229.5	131.0	90.5	0.0	1.0	3.0	57.1	39.4	0.0	0.4	1.3	6.5	6.0	–	–	0.9
0.5–1.0	107.5	55.0	46.0	0.0	2.0	2.0	51.2	42.8	0.0	1.9	1.9	9.0	9.5	–	1.5	1.5
1.0–2.0	113.0	50.5	51.5	0.0	3.0	7.0	44.7	45.6	0.0	2.7	6.2	9.0	9.0	–	2.0	4.0
2.0–3.0	146.0	60.5	42.0	10.0	3.0	26.0	41.4	28.8	6.8	2.1	17.8	8.0	7.5	3.5	1.6	6.0
3.0–4.0	134.0	37.5	22.5	15.0	10.0	32.0	28.0	16.8	11.2	7.5	23.9	8.0	6.0	5.0	4.0	7.0
4.0–5.0	181.0	67.0	51.5	9.0	15.0	25.0	37.0	28.5	5.0	8.3	13.8	7.0	6.5	3.0	4.0	5.0
5.0–7.5	83.0	22.0	19.0	9.0	10.0	8.5	26.5	22.9	10.8	12.0	10.2	9.0	8.5	5.5	6.0	5.5
7.5–10.0	137.5	40.0	36.0	18.0	6.0	28.0	29.1	26.2	13.1	4.4	20.4	8.0	7.0	6.0	3.5	6.5

https://doi.org/10.1016/j.yqres.2012.04.001 Published online by Cambridge University Press

Table 4
List of S- and R-cysts (after Zonneveld et al., 1997, 2001; Bockelmann, 2007; Esper and Zonneveld, 2007).

Sensitive dinocysts (S-cysts)	Resistant dinocysts (R-cysts)
Brigantedinium spp.	*Impagidinium aculeatum*
Selenopemphix antarctica	*Impagidinium patulum*
Echinidinium spp.	*Impagidinium sphaericum*
Cyst of *Protoperidinium* spp.	*Impagidinium plicatum*
	Impagidinium strialatum
	Impagidinium spp.
	Namatosphaeropsis labyrinthus
	Operculodinium centrocarpum
	Operculodinium israelianum
	Spiniferites spp.

Schlüter et al. (1998) discovered biogenic silica production and rain rates to be two and ten times higher respectively in the PF region (Scotia Sea and eastern Antarctic Circumpolar Current) in comparison to other areas of the SO. In addition, coupling of primary production and OC rain rates was suggested for some areas of the SO that may be related to export efficiency of OC and biogenic silica from the euphotic zone, and to differences in remineralisation and dissolution processes in the water column (Schlüter et al., 2000). Elevated sedimentation rates had already been reported for deposits of different ages from a variety of locations in the SO. For example, Frank et al. (1996) described sedimentation rates of up to 0.033 cm/yr in the Late Quaternary deposits from the Atlantic sector of the SO. Pudsey and Howe (1998) and Howe et al. (2002) reported sedimentation rates of up to 0.017 and 0.026 cm/yr in Holocene and Last Glacial Maximum sediments from the Scotia Sea. For the sediments from Marine Oxygen Isotope Stage (MIS) 1 in the SO, sedimentation rates of up to 0.064 cm/yr were calculated (Levitan and Stein, 2008). Additionally, sedimentation rates of up to 0.025 cm/yr were estimated for surface sediments in the PF region of the Indian Ocean (Fagel, 2006).

Core 705

Fifteen dinocyst taxa were encountered out of which 4 taxa made up 80–99% of the dinocyst associations. Heterotrophic S-cysts *Brigantedinium* spp. and *Selenopemphix antarctica* made up 40–70% and 20–40% of the association respectively. Autotrophic R-cysts *Nematosphaeropsis labyrinthus* and *Impagidinium sphaericum* constituted generally 2–15% and 8–35% of the dinocyst assemblages respectively. Other species never reached the 5% abundance level except for *Dalella chathamensis* and *Impagidinium aculeatum* the percentages of which rose periodically up to 7% each (Fig. 3a).

The bottom of the core was characterised by low *Brigantedinium* spp. and *S. antarctica* fluxes, which then increased in the interval from 1901 to 1950 AD. Later in the record they decreased again to reach the lowest values in the 1950–1978 AD interval. Gradual recovery of the fluxes was observed towards the top of the core, reaching the highest levels in samples representing 2000 and

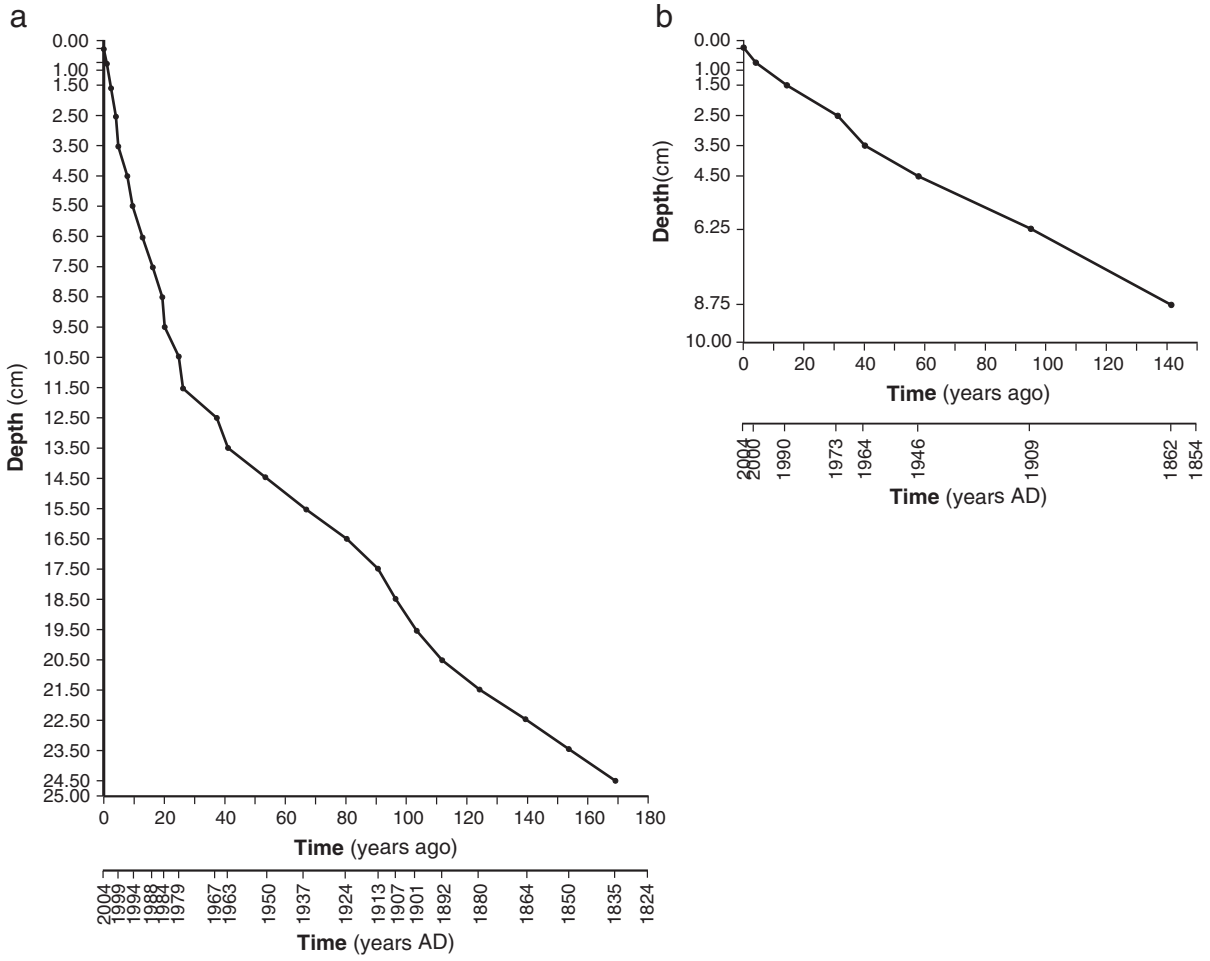

Figure 2. Relation between sediment depth (cm) and the sample age (in yr ago and yr AD) in a) core 705 and b) core 703.

https://doi.org/10.1016/j.yqres.2012.04.001 Published online by Cambridge University Press

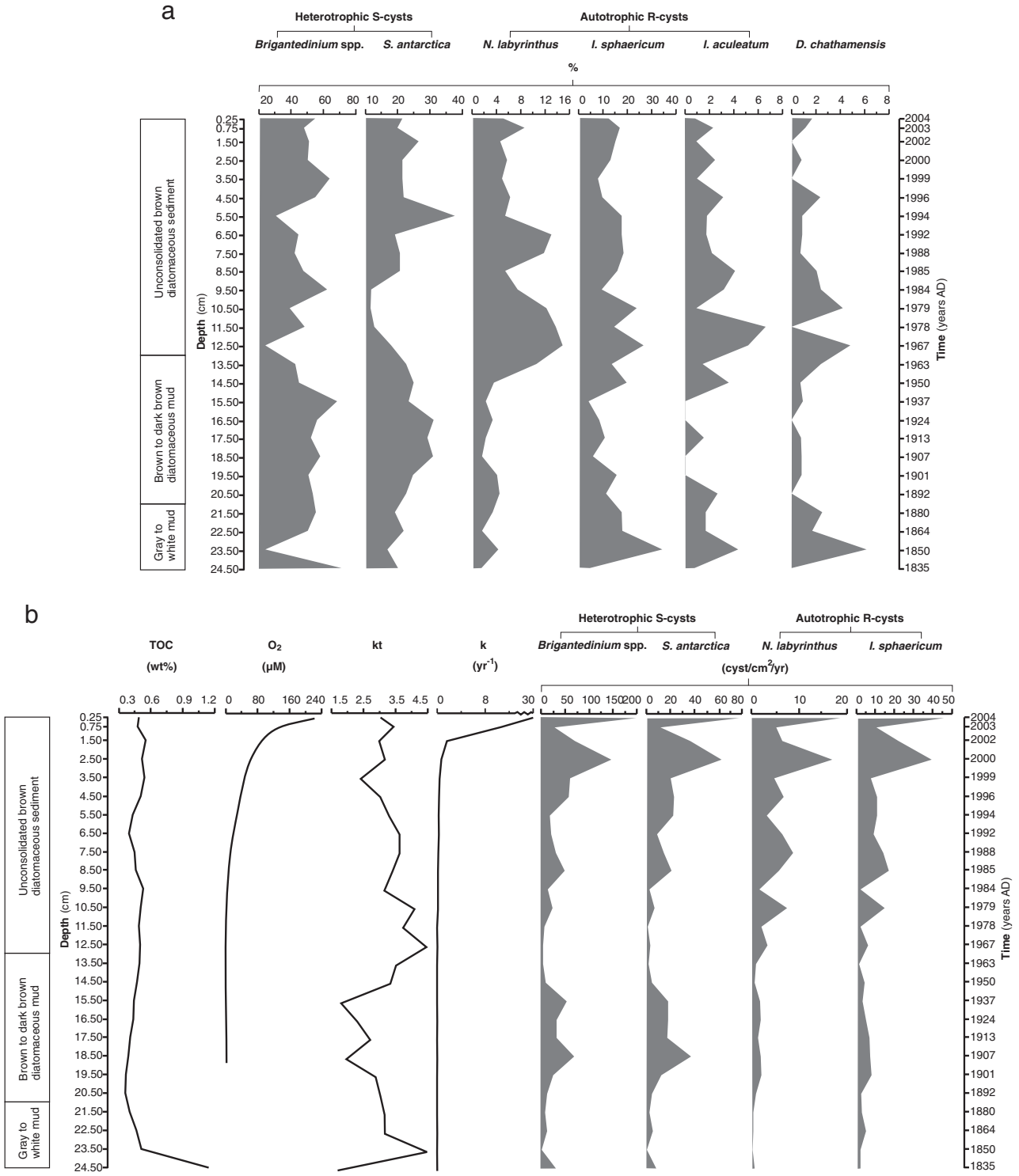

Figure 3. a) Percentages of selected dinocyst taxa and b) TOC, pore-water O_2 concentrations and fluxes of selected dinocyst taxa in core 705.

2004 AD (Fig. 3b). *N. labyrinthus* and *I. sphaericum* displayed lowest fluxes (1–2 and 2–5 cyst/cm^2/yr respectively) in the lowermost samples. Their fluxes gradually increased towards the top of the core reaching maximum values (17–18, and 38–45 cyst/cm^2/yr respectively) in the samples from 2000 and 2004 AD (Fig. 3b).

TOC ranged from 0.35 to 0.55% with generally lower values in the lower part of the core and higher in the middle, followed by a decrease until 1992 AD and a subsequent recovery towards the top of the core (Fig. 3b).

Values of the *kt* index ranged generally from 3 to 4 throughout the core. Samples from 1850 and 1967 AD have a $kt > 4$ whereas samples dated to 1835, 1907 and 1937 AD display a $kt < 2$. The *k* values in the anoxic part of the core ranged from 0.01 to 0.10 yr^{-1} without a significant trend. In the oxygenated part of the core *k* increased upwards from 0.16 up to 30 yr^{-1}. Pore-water O_2 decreased down-core from 225 μM at the sediment surface to oxygen depletion below 9 cm depth (Fig. 3b). *k* is exponentially related to the pore-water O_2 concentration according to the equation: $y = 0.1449e^{0.0336k}$, $R^2 = 0.9726$ (Fig. 4).

https://doi.org/10.1016/j.yqres.2012.04.001 Published online by Cambridge University Press

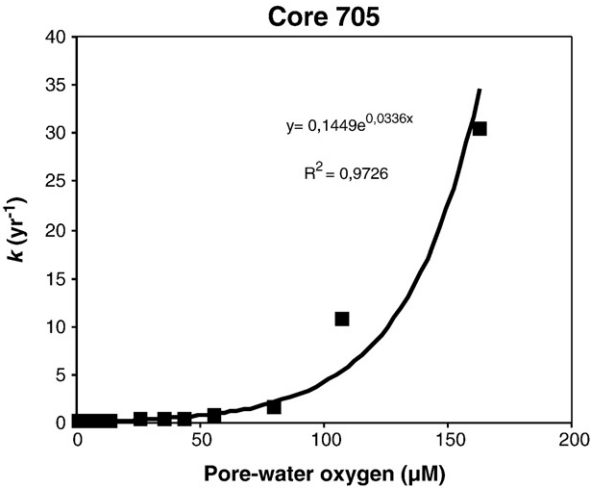

Figure 4. Relation between degradation constant *k* and pore-water O_2 concentrations in core 705.

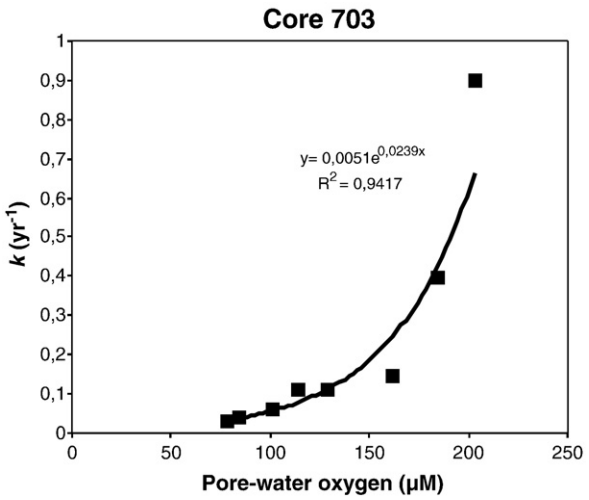

Figure 6. Relation between degradation constant *k* and pore-water O_2 concentrations in core 703.

Core 703

Fourteen dinocyst taxa were encountered during counting, out of which four taxa made up 80–98% of the dinocyst assemblages. The heterotrophic S-cysts *Brigantedinium* spp. and *S. antarctica* made up 27–57% and 17–45% of the association respectively. The autotrophic R-cysts *I. sphaericum* and *I. aculeatum* made up 1–24% and 0.5–12% of the dinocyst associations. Another R-cyst, *N. labyrinthus*, was absent in the upper part of the core but present in the lower part, where it contributed 5–13% of the dinocyst assemblage (Fig. 5a).

Fluxes of S-cysts increased from 0.5 to about 100 cyst/cm^2/yr towards the top of the core. Fluxes of R-cysts remained rather constant throughout the core (Fig. 5b).

TOC was measured only for the upper 4 cm of the core and increased slightly but continuously up-section from 0.38 to 0.48% (Fig. 5b).

The values of the *kt* index decreased generally from 4 at the bottom to 1 at the top of the core. The degradation constant *k* increased upwards from 0.03 up to 0.90 yr^{-1}. Pore-water O_2 decreased downcore from 213 μM at the sediment surface to 112 μM at 8 cm depth

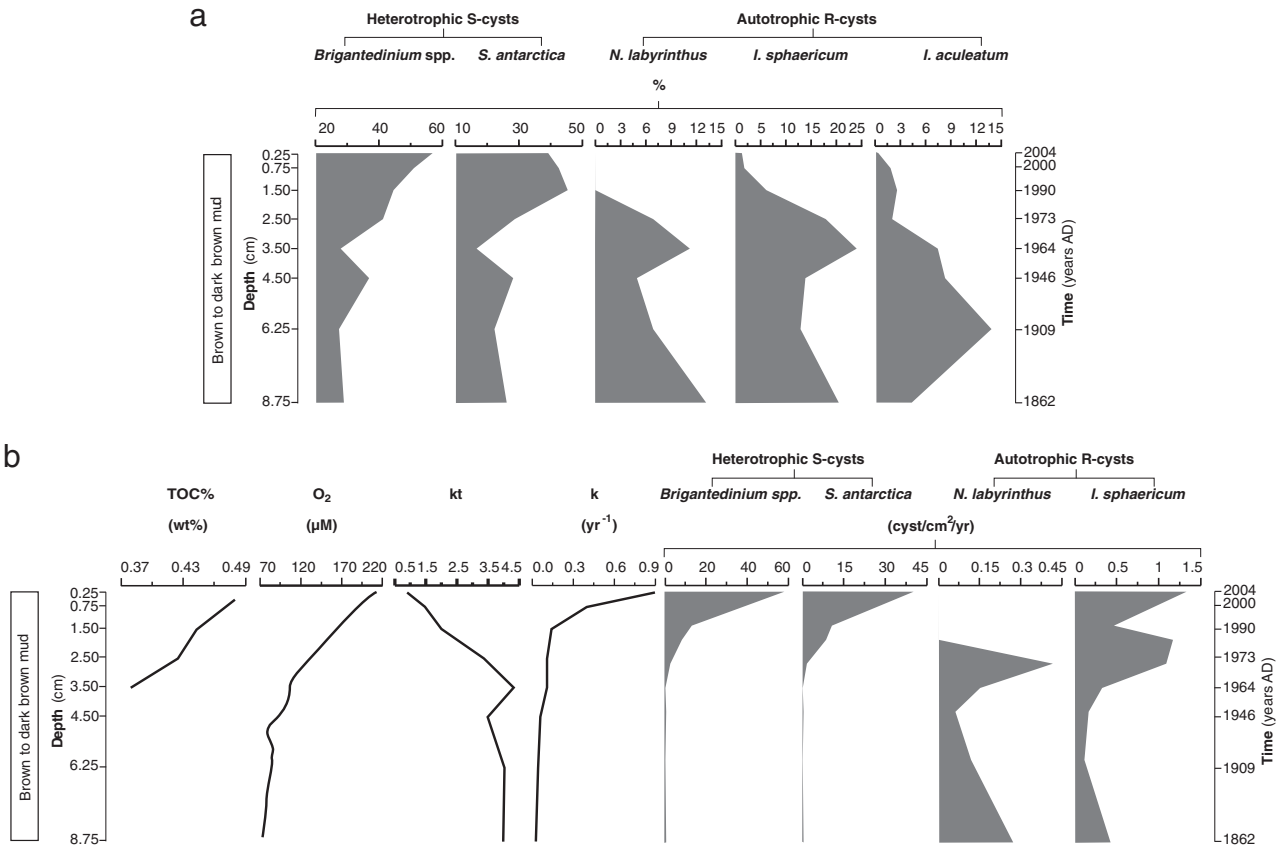

Figure 5. a) Percentages of selected dinocyst taxa and b) TOC, pore-water O_2 concentrations and fluxes of selected dinocyst taxa in the core 703.

https://doi.org/10.1016/j.yqres.2012.04.001 Published online by Cambridge University Press

(Fig. 5b). *k* decreases exponentially with decreasing pore-water O_2 concentration according to the equation: $y = 0.0051e^{0.0239k}$, $R^2 = 0.9417$ (Fig. 6).

Discussion

The dinocyst associations in both cores are dominated by the heterotrophic S-cysts *Brigantedinium* spp. and *S. antarctica*; autotrophic R-cysts *I. sphaericum* and *N. labyrinthus* are present but less abundant. Our dinocyst assemblages are, therefore, reminiscent of late Quaternary and recent assemblages from the northern part of the SO (Esper and Zonneveld, 2002, 2007), and of the southerly subunit of dinocyst associations north of 60°S described by Harland et al. (1998) for core-top samples from the Scotia Sea and the Falkland Trough. Sediment trap studies from the Scotia Sea also indicated associations dominated by *Brigantedinium* spp. and *S. antarctica* with a minor component of autotrophic dinocysts (Harland and Pudsey, 1999). The dominance of heterotrophic species in the assemblage is in agreement with the cores locations both at (705) and to the south (703) of the PF, since heterotrophic dinoflagellates are known to feed predominantly on diatoms (Jacobson and Anderson, 1986), and upwelling along the PF is characterised by very high diatom abundances (Zielinski and Gersonde, 1997). Increased heterotrophic dinoflagellate growth was also recently associated with the diatom productivity in the western Canadian Arctic Shelf region (Richerol et al., 2008).

The core 705 spans 170 yr from 1835 to 2004 AD. However, the lower half of the studied section was deposited over a relatively long period of 145 yr, in contrast with the upper half deposited during a short period of 25 yr. This upper part comprises the inhomogeneous and bioclastic, extremely soft layer of diatomeous mud and is hypothesised to be relatively rapidly deposited during prolonged periods of enhanced sedimentation in comparison to the rest of the core (Sachs, 2008). Indeed, sedimentation rates are generally lower for the lower half (0.06–0.22 cm/yr) than for the upper half of the core (0.29–1.56 cm/yr). Such a subdivision of the core is therefore also reflected in the dinocyst flux pattern, with low fluxes occurring in the lower part of the core and increased fluxes in the upper part.

The bottom of core 705 (1835–1901 AD) is characterised by very low fluxes of dinocysts. It is followed by an interval (1901–1950 AD) of higher fluxes of heterotrophic dinocysts and low fluxes of autotrophic dinocysts (Fig. 3b). The heterotrophs depend on prey availability (e.g. diatoms, protists) therefore they are very abundant in high-productivity areas such as, for example, upwelling regions (Harland et al., 1998). Additionally *S. antarctica* is associated with cold water masses and the proximity of seasonal sea-ice cover (Marret and de Vernal, 1997; Harland et al., 1999). Increased fluxes of the heterotrophs could indicate a northerly shift of the PF (Howe et al., 2002) and, concomitantly, a high-productivity upwelling area. A displacement of these features would result not only in higher prey availability, and therefore better conditions for heterotrophic species growth but also in lower sea-surface temperatures and proximity of the maximum sea-ice limit — exactly the conditions favourable for *S. antarctica*. In the upper part of core 705 (1950–1979 AD), at the interface between more solid and extremely soft sediment, the fluxes and percentages of heterotrophic dinocysts decrease again to their lowest level. This coincides with a sharp peak in percentages of autotrophic dinocysts although peaks of similar magnitude were not observed for fluxes. In polar domains the autotrophs *N. labyrinthus* and *I. sphaericum* are interpreted as representative of relatively warmer water masses and permanently ice-free conditions (McMinn et al., 2001; Howe et al., 2002). This, in contrast to the previous interval, might suggest a southern shift of the PF and the introduction of higher sea-surface temperatures. This is further supported by increased percentages of another two species, *D. chathamense* and *I. aculeatum*, that are thought to be associated with relatively warmer waters (Marret and de Vernal, 1997; McMinn et al., 2001).

Farther up the core (1979–2004 AD) the fluxes of heterotrophic S-cysts increase again to reach approximately the same values as in the 1901–1950 AD interval (with the exception of samples from 2000 and 2004 AD for which fluxes reached even higher values). This would indicate a return to a more northerly location of the PF and the associated high-productivity belt. The prominent feature of this section is a short-term (1992–1996 AD) shift to *S. antarctica*-dominated assemblages that is generally indicative of colder conditions, since this dinocyst is associated with cold water masses and the proximity of seasonal sea-ice cover (Marret and de Vernal, 1997; Harland et al., 1999). In our core, this interval suggests the coldest sea-surface conditions within the studied period. This hypothesis is further corroborated by sea-ice concentration data collected by NOAA (www.cdc.noaa.gov). The sea-ice concentration averaged over the period 1992–1996 AD shows a northerly shift (by 1°) of the maximum sea-ice limit in comparison to times before and after this period.

However, higher fluxes of heterotrophic S-cysts in the 1901–1950 AD period, as well as lower fluxes in the 1950–1979 AD interval, may be related not only to changes in palaeoenvironment but also to species-selective preservation/degradation of these dinocysts under aerobic conditions as suggested by lower (<2) and higher (>4) *kt* values respectively, in comparison to the other samples ($3 < kt < 4$). OC degradation, and hence also dinocyst degradation, is assumed to manifest a first-order dependence on the reactivity of OC and *t* (Middelburg, 1989; Canfield, 1994; Hartnett et al., 1998; Sun et al., 2002; Keil et al., 2004). In core 705 the degradation index *kt* is relatively constant through time. Samples with assumed *t* of only a few years experienced the same degree of degradation as samples exposed to O_2 for 25 yr. That would suggest that degradation in this case depends on factors other than *t*. Throughout the entire core, and especially in the upper half, there were high abundances of S-cysts preserved in the sediment. Hence, the availability of labile OC does not seem to be the limiting factor for the degradation. However, in this case O_2 is consumed much faster, resulting in oxygen-depleted conditions in the lower part of the sediments, and thus pointing to the limiting role of the O_2. The calculated constant *k* for the oxic part of the core correlates well with pore-water O_2 concentrations. This would suggest a dependence of OC degradation on O_2 concentrations. Recently Zonneveld et al. (2007) found a significant relationship between dinocyst degradation and bottom-water O_2 concentrations. This supports our observations since pore-water O_2 concentrations are dependent, amongst other factors, on the concentration of bottom-water O_2 that diffuses downwards into sediments. Furthermore, Bockelmann (2007) concluded that dinocyst degradation is dependent on the bottom-water O_2 concentrations until a critical O_2 level of ~3 ml/l: above this level degradation seems to be controlled by the flux of S-cysts. Due to rapid oxygen depletion in the sediments of core 705, a considerable amount of S-cysts could have been escaped degradation. As pointed out earlier, the relatively uniform *kt* index throughout the core suggest that dinocyst associations in all samples were affected by selective preservation at the same level and hence their pattern, but not their absolute numbers, can be interpreted in terms of palaeoenvironmental changes. The exception may be the few samples with higher or lower *kt* values than the average. If samples with these differing *kt* values are excluded from the analysis, the whole interval 1901–1979 seems to have much more stable dinocyst fluxes and indicate stable palaeoceanographic conditions.

Core 703 spans 142 yr from 1862 to 2004 AD. Sedimentation rates were again lower (0.03–0.05 cm/yr) in the lower half of the core in comparison to the upper half (0.05–0.13 cm/yr). The dinocyst fluxes increase towards the top of the core as does TOC; however, percentages of individual dinocyst species behave differently. Percentages of S-cysts increase upwards while R-cysts percentages decrease

https://doi.org/10.1016/j.yqres.2012.04.001 Published online by Cambridge University Press

upwards although their fluxes increase. Such dinocyst trends are characteristic for assemblages affected by species-selective aerobic degradation. The decomposition of the S-cysts could cause an increase in the percentages of the R-cysts (e.g. Zonneveld et al., 1997, 2001; Hopkins and McCarthy, 2002; Reichart and Brinkhuis, 2003; Esper and Zonneveld, 2007; Kodrans-Nsiah et al., 2008). The continuous decrease of the calculated *kt* index towards the top of the core supports the hypothesis of selective degradation and hints at much better dinocyst preservation in the upper part than in the lower part of the core. We therefore conclude that in this case, the dinocyst record is the result of species-selective aerobic degradation instead of changes in primary productivity or in paleoceanographic conditions.

In situ pore-water O_2 concentration measurements at the core 703 site indicate oxic conditions throughout the core. Under the assumption of a steady state situation the age of our samples would mirror the *t* with the bottom sample being exposed to O_2 for 142 yr and the top samples for only a few years. Thus it is not surprising that dinocyst preservation should be worse in the lower part than the upper part of the core. The calculated degradation constant *k* increases with decreasing *t* which supports the statement that degradation depends on the reactivity of OC. The most reactive OC is degraded quickly whereas the degradation of less reactive components proceeds slowly over a longer time. In our case the most sensitive dinocysts are decomposed within the upper 3 cm of the core (corresponding to ~30 yr of *t*), however degradation of the less sensitive dinocysts proceeds over the longer time period at slower rates which are indicated by lower *k* values. The *k* also correlates positively with measured pore-water O_2 concentrations implying that the degradation is dependent not only on the presence/absence of the O_2 but also on the O_2 concentration. As O_2 diffuses from the bottom water into the sediment it is ultimately consumed by OC degradation. A certain amount of O_2 can oxidise only a limited amount of OC. In this case an average of 0.03 mol O_2 per m^2/yr can oxidise up to 0.25 g C per m^2/yr (calculated according to Fick's First Law and OC:O_2 ratio 106:138; Froelich et al., 1979; Schulz, 2005). Accordingly, higher O_2 concentrations would cause the degradation of a larger amount of OC in the same period of time. Less reactive OC and lower O_2 levels would cause a decreasing *k* with an increasing *t*. However, although O_2 is available throughout the whole length of the core, degradation seems not to change significantly over the lower 7 cm which would imply that although degradation is dependent on the O_2 concentration, here the final limiting factor might be availability of the reactive components, as the amount of labile dinocysts in the lower part of the core nears zero.

Dinocysts are one of the significant constituents of marine OC and, therefore, their decomposition is based on the same premises as degradation of the entire OC pool. The OC degradation in marine sediments is widely believed to be a first-order process dependent on the labile OC concentration and *t* (Middelburg, 1989; Hedges and Prahl, 1993; Canfield, 1994; Hartnett et al., 1998; Sun et al., 2002; Keil et al., 2004). In general, sediments with longer *t* have lower OC contents, as well as lower OC burial efficiencies (Hartnett et al., 1998). This is also true for dinocysts. In core 703, samples with longer *t* have experienced more severe degradation, and as a result contain many fewer dinocysts than samples with shorter *t*. The samples from the top of the core contain high numbers of S-cysts and therefore are characterised by high *kt* index values, suggesting rapid degradation where vast amounts of labile components are present. Sedimentation rate also exerts a strong influence on burial efficiency, with increased sedimentation rates enhancing preservation of deposited OC (Henrichs and Reeburgh, 1987; Betts and Holland, 1991; Tromp et al., 1995). We also observed better preservation of dinocysts in the samples with estimated higher sedimentation rates. Some authors additionally argue that degradation of OC depends on the O_2 concentrations in pore waters (Berner, 1980; Rabouille and Gaillard, 1991; Cai and Sayles, 1996), suggesting the same higher-order kinetics for decomposition processes. Emerson (1985) showed low OC burial efficiencies in the presence of high bottom-water O_2 concentration whereas Hartnett et al. (1998) described the highest burial efficiencies in regions with undetectable bottom-water O_2. Higher-order kinetics for dinocyst degradation processes have already been hypothesised by Zonneveld et al. (2007). This hypothesis is supported by dinocysts recorded from core 705 where dinocyst degradation in samples with long *t* and availability of labile OC (S-cysts) proceeds with generally equal rates to the samples with shorter *t* because of decreasing pore-water O_2 concentrations with increasing depth. The OC pool consists of labile and refractory components mixed together which are selectively aerobically decomposed. Dinocysts associations are, in turn, composed of sensitive and resistant species and degraded in a similarly selective way. Dinocyst decomposition shows a dependence on the amount of labile components (S-cysts), *t* and pore- and bottom-water O_2 concentrations. If we assume higher-order kinetics for the OC degradation process we may use then dinocyst taphonomy as a model for studies on decomposition of the entire OC pool.

Conclusion

Both cores are characterised by low dinocyst fluxes that, at least partially, may be the result of selective degradation of heterotrophic S-cysts. Our results indicate that early diagenesis may significantly influence the primary fossil signal and, as in the case of core 703, prevent the recognition of palaeoenvironmental changes. In such cases dinocyst-based methods for palaeoenvironmental reconstructions, for example transfer functions, should be used with caution.

The relationship between calculated *k* values and pore-water O_2 concentrations suggests that the degradation of OC is dependent on the bottom- and pore-water O_2 concentration as well as on the labile OC fraction and *t*. The O_2 concentration seems to be a more important limiting factor for diagenetic processes at lower O_2 concentrations, whereas at higher O_2 levels the availability of reactive OC is crucial.

Recognition of the selective degradation may lead to differentiation between primary and overprinted signals, and hence may enable the accurate palaeoenvironmental interpretation of fossil records as demonstrated for core 705.

Acknowledgments

We thank Timothy G. Ferdelman (MPI, Bremen) and Ian C. Harding (NOC, Southampton) for helpful consultations. This study was supported by DFG grant EUROPROX.

References

Aller, R.C., 2001. Transport and reactions in the bioirrigated zone. In: Boudreau, B.P., Jørgensen, B.B. (Eds.), The Benthic Boundary Layer. Oxford University Press, Oxford, pp. 269–301.
Aller, R.C., Blair, N.E., 2006. Carbon remineralization in the Amazon-Guianas tropical moile mudbelt: a sedimentary incinerator. Continental Shelf Research 26 (17–18), 2241–2259.
Arthur, M.A., Dean, W.E., Laarkamp, K., 1998. Organic carbon accumulation and preservation in surface sediments on the Peru margin. Chemical Geology 152, 273–286.
Barnett, P.R.O., Watson, J., Conelly, D., 1984. A multiple corer for taking virtually undisturbed samples from shelf, bathyal, and abyssal sediments. Oceanologica Acta 7, 399–408.
Berner, R.A., 1980. Early Diagenesis: A theoretical Approach. Princeton University Press, Princeton, New Jersey.
Betts, J.N., Holland, 1991. The oxygen content of ocean bottom waters, the burial efficiency of organic carbon and the regulation of atmospheric oxygen. Global and Planetary Change 97, 5–18.
Bockelmann, F.-D., 2007. Selective preservation of organic-walled dinoflagellate cysts in Quaternary marine sediments: An oxygen effect and its application to paleoceanography. PhD Thesis, University of Bremen, 130 pp.
Cai, W.-J., Sayles, F.L., 1996. Oxygen penetration depths and fluxes in marine sediments. Marine Chemistry 52, 123–131.
Canfield, D.E., 1994. Factors influencing organic carbon preservation in marine sediments. Chemical Geology 114, 315–329.
Emerson, S.E., 1985. Organic carbon preservation in marine sediments. In: Sundquist, E.T., Broecker, W.S. (Eds.), The Carbon Cycle and Atmospheric CO_2: Natural

Variations Archean to Present. : Geophysical Monographs, 32. American Geophysical Union, Washington, D. C.
Esper, O., Zonneveld, K.A.F., 2002. Distribution of organic-walled dinoflagellate cysts in surface sediments of the Southern Ocean (eastern Atlantic sector) between the Suptropical Front and the Weddell Gyre. Marine Micropaleontology 46, 177–208.
Esper, O., Zonneveld, K.A.F., 2007. The potential of organic-walled dinoflagellate cysts to reconstruct past sea-surface conditions in the Southern Ocean. Marine Micropaleontology 65 (3/4), 185–212.
Fagel, N., 2006. Export Production Estimates for the Surface Sediments in the Atlantic and Indian Sectors of the Southern Ocean (Table 3,4). http://dx.doi.org/10.1594/PANGAEA.464582.
Ferdelman, T.G., Thamdrup, B., Canfield, D.E., Nøhr Glud, R., Kuever, J., Lillebæk, R., Birger Ramsing, N., Wawer, C., 2006. Biogeochemical controls on the oxygen, nitrogen and sulfur distributions in the water column of Golfo Dulce: an anoxic basin on the Pacific coast of Costa Rica revisited. Revista de Biología Tropical 54, 171–191.
François, R., Altabet, M.A., Yu, E.-F., Sigman, D.M., Bacon, M.P., Frank, M., Bohrmann, G., Bareille, G., Labeyrie, L.D., 1997. Contribution of Southern Ocean surface-water stratification to low atmospheric CO_2 concentrations during last glacial period. Nature 389, 929–935.
Frank, M., Mangini, A., Gersonde, R., Rutgers vander Loeff, M., Kuhn, G., 1996. Late Quaternary sediment dating and quantification of lateral sediment redistribution applying $^{230}Th_{ex}$: a study from the eastern Atlantic sector of the Southern Ocean. Geologische Rundschau 85 (3), 554–566.
Froelich, P.N., Klinkhammer, G.P., Bender, M.L., Luedtke, N.A., Heath, G.R., Cullen, D., Dauphin, P., Hammond, D., Hartman, B., Maynard, V., 1979. Early oxidation of organic matter in pelagic sediments of the eastern equatorial Atlantic: suhoxic diagenesis. Geochimica et Cosmochimica Acta 43, 1075–1090.
Harland, R., Pudsey, C.J., 1999. Dinoflagellate cysts from sediment traps deployed in the Bellingshausen, Weddell and Scotia seas, Antarctica. Marine Micropaleontology 37, 77–99.
Harland, R., Pudsey, C.J., Howe, J.A., Fitzpatrick, M.E., 1998. Recent dinoflagellate cysts in a transect from the Falkland Trough to the Weddell Sea, Antarctica. Palaeontology 41 (6), 1093–1131.
Harland, R., Fitzpatrick, M.E.J., Pudsey, C.J., 1999. Latest Quaternary dinoflagellate cyst climatostratigraphy for three cores from the Falkland Trough, Scotia and Weddell seas, Southern Ocean. Review of Palaeobotany and Palynology 107, 265–281.
Hartnett, H.E., Keil, R.G., Hedges, J.I., Devol, A.H., 1998. Influence of oxygen exposure time on organic carbon preservation in continental margin sediments. Nature 391, 572–574.
Hedges, J.I., Prahl, F.G., 1993. Early diagenesis: consequences for applications of molecular biomarkers. In: Engel, M.H., Macko, S.A. (Eds.), Organic Geochemistry. Plenum Press, New York.
Hedges, J.I., Keil, R.G., Benner, R., 1997. What happens to terrestrial organic matter in the ocean? Organic Geochemistry 27 (5–6), 195–212.
Henrichs, S.M., Reeburgh, W.S., 1987. Anaerobic mineralization of marine sediment organic matter: rates and the role of anaerobic processes in the oceanic carbon economy. Geomicrobiology Journal 5, 191–237.
Hopkins, J.A., McCarthy, F.M.G., 2002. Post-depositional palynomorph degradation in Quaternary shelf sediments: a laboratory experiment studying the effects of progressive oxidation. Palynology 26, 167–184.
Howarth, R.J., 1998. Improved estimators of uncertainty in proportions, point-counting, and pass-fail test results. American Journal of Science 298, 594–607.
Howe, J.A., Harland, R., Pudsey, C.J., 2002. Dinoflagellate cysts evidence for Quaternary palaeoceanographic change in the northern Scotia Sea, South Atlantic Ocean. Marine Geology 191, 55–69.
Hulthe, G., Hulth, S., Hall, P.O.J., 1998. Effect of oxygen on degradation rate of refractory and labile organic matter in continental margin sediments. Geochimica et Cosmochimica Acta 62 (8), 1319–1328.
Jacobson, D.M., Anderson, D.M., 1986. Thecate heterotrophic dinoflagellates: feeding behavior and mechanisms. Journal of Phycology 22, 249–258.
Keil, R.G., Dickens, A.F., Arnarson, T., Nunn, B.L., Devol, A.H., 2004. What is the oxygen exposure time of laterally transported organic matter along the Washington margin? Marine Chemistry 92, 157–165.
Kodrans-Nsiah, M., de Lange, G.J., Zonneveld, K.A.F., 2008. A natural exposure experiment on short-term species-selective aerobic degradation of dinoflagellate cysts. Review of Palaeobotany and Palynology 152, 32–39.
Levitan, M.A., Stein, R., 2008. History of sedimentation rates in the sea-ice sedimentation zone during the last 130 ka. Lithology and Mineral Resources 43 (1), 65–75.
Marret, F., de Vernal, A., 1997. Dinoflagellate cysts distribution in surface sediments of the southern Indian Ocean. Marine Micropaleontology 29, 367–392.
Martin, J.H., Fitzwater, S.E., Gordon, R.M., 1990. Iron deficiency limits phyto-plankton growth in the Antarctic waters. Global Biogeochemical Cycles 4, 5–12.
McMinn, A., Howard, W.R., Roberts, D., 2001. Late Pliocene dinoflagellate cysts and diatom analysis from a high resolution sequence in DSDP Site 594, Chatham Rise, south west Pacific. Marine Micropaleontology 43, 207–221.
Middelburg, J.J., 1989. A simple rate model for organic matter decomposition in marine sediments. Geochimica et Cosmochimica Acta 53, 1577–1581.
Moore, J.K., Abbott, M.R., Richman, J.G., Nelson, D.M., 2000. The Southern Ocean at the last glacial maximum: a strong sink for atmospheric carbon dioxide. Global Biogeochemical Cycles 14, 455–475.
Pudsey, C.J., Howe, J.A., 1998. Quaternary history of the Antarctic Circumpolar Current: evidence from the Scotia Sea. Marine Geology 148, 83–112.
Rabouille, C., Gaillard, J.-F., 1991. A coupled model representing the deep-sea organic carbon mineralization and oxygen consumption in surficial sediments. Journal of Geophysical Research 96 (C2), 2761–2776.
Reichart, G.-J., Brinkhuis, H., 2003. Late Quaternary Protoperidinium cysts as indicators of paleoproductivity in the northern Arabian Sea. Marine Micropaleontology 49, 303–315.
Richerol, T., Rochon, A., Blasco, S., Scott, D.B., Schell, T.M., Bennett, R.J., 2008. Distribution of dinoflagellate cysts in surface sediments of the Mackenzie Shelf and Amundsen Gulf, Beaufort Sea (Canada). Journal of Marine Systems, http://dx.doi.org/10.1016/j.jmarsys.2007.11.003.
Robbins, J.A., 1978. Geochemical and geophysical applications of radioactive lead. In: Nriagu, J.O. (Ed.), The Biogeochemistry of Lead in the Environment. Part A. Ecological Cycles. Elsevier, pp. 285–393.
Sachs, O., 2008. Benthic organic carbon fluxes in the Southern Ocean: regional differences and links to surface primary production and carbon export. Reports on Polar and Marine Research, 578. 158 pp.
Sauter, E.J., Schlüter, M., Suess, M., 2001. Organic carbon flux and remineralization in surface sediments from the northern North Atlantic derived from pore-water oxygen microprofiles. Deep-Sea Research I 48, 529–553.
Schlüter, M., Rutgers van der Loeff, M.M., Holby, O., Kuhn, G., 1998. Silica cycle in surface sediments of the South Atlantic. Deep Sea Research 45, 1085–1109.
Schlüter, M., Sauter, E.J., Schulz-Bull, D., Balzer, W., Suess, E., 2000. Fluxes of organic carbon and biogenic silica reaching the seafloor: a comparison of high northern and southern latitudes of the Atlantic Ocean. In: Schäfer, P., Ritzrau, W., Schlüter, M., Thiede, J. (Eds.), The Northern North Atlantic: A Changing Environment. Springer, Berlin, pp. 225–240.
Schulz, H.D., 2005. Quantification of early diagenesis: dissolved constituents in pore water and signals in the solid phase, In: Schulz, H.D., Zabel, M. (Eds.), Marine Geochemistry, 2nd Edition. Springer, Verlag Brelin Heidelberg, pp. 73–124.
Siegenthaler, U., Wenk, T., 1984. Rapid atmospheric CO_2 changes and ocean circulation. Nature 308, 624–626.
Sigman, D.M., Boyle, E.A., 2000. Glacial/interglacial variations in atmospheric carbon dioxide. Nature 407, 859–869.
Sun, M.-Y., Cai, W.-J., Joye, S.B., Ding, H., Dai, J., Hollibaugh, J.T., 2002. Degradation of algal lipids in microcosm sediments with different mixing regimes. Organic Geochemistry 33, 445–459.
Tromp, T.K., van Cappellen, P., Key, R.M., 1995. A global model for the early diagenesis of organic carbon and organic phosphorus in marine sediments. Geochimica et Cosmochimica Acta 59 (7), 1259–1284.
Van der Plas, L., Tobi, A.C., 1965. A chart for judging the reliability of point counting results. American Journal of Science 263, 87–90.
Versteegh, G.J.M., Zonneveld, K.A.F., 2002. Use of selective degradation to separate preservation from productivity. Geology 30 (7), 615–618.
Zielinski, U., Gersonde, R., 1997. Diatom distribution in Southern Ocean surface sediments (Atlantic sector): implications for paleoenvironmental reconstructions. Palaeogeography, Palaeoclimatology, Palaeoecology 129, 213–250.
Zonneveld, K.A.F., Versteegh, G.J.M., de Lange, G.J., 1997. Preservation of organic-walled dinoflagellate cysts in different oxygen regimes: a 10,000 year natural experiment. Marine Micropaleontology 29, 393–405.
Zonneveld, K.A.F., Versteegh, G.J.M., de Lange, G.J., 2001. Palaeoproductivity and post-depositional aerobic organic matter decay reflected by dinoflagellate cyst assemblages of the Eastern Mediterranean S1 sapropel. Marine Geology 172, 181–195.
Zonneveld, K.A.F., Bockelmann, F., Holzwarth, U., 2007. Selective preservation of organic walled dinoflagellate cysts as a tool to quantify past net primary production and bottom water oxygen concentrations. Marine Geology 237, 109–126.
Zonneveld, K.A.F., Versteegh, G., Kodrans-Nsiah, M., 2008. Preservation and organic chemistry of late Cenozoic organic-walled dinofalgellate cysts; a review. Marine Micropaleontology 68 (1/2), 179–197.